Soft Matter

RSC Publishing

PAPER

Magnetorheology from surface coverage of spin-coated colloidal films†

Cite this: *Soft Matter*, 2013, **9**, 2506

Moorthi Pichumani‡ and Wenceslao González-Viñas*

In magnetorheological fluids, the viscosity usually increases with the field and the non-Newtonian character of these complex fluids may vary significantly. We provide a new method to measure the relative viscosity of a superparamagnetic colloid, by applying a magnetic field during a spin-coating process, which involves evaporation of the solvent. We define the compact equivalent height to take into account the discrete nature of the suspension, and we compare experimental results under different conditions. We extend the model of Cregan *et al.* (*J. Colloid Interface Sci.*, 2007, **314**, 324) to turn it into an evaporation rate independent one. The generality of the resulting model facilitates measurement of the magnetic field dependent viscosity. We also discuss the morphologies of the final dried colloidal deposits and the possible mechanisms involved in their formation.

Received 20th November 2012
Accepted 18th December 2012

DOI: 10.1039/c2sm27682h

www.rsc.org/softmatter

1 Introduction

Spin-coating of polymer solutions[1–3] has brought commercial advances in manufacturing devices for electronic applications. Recently, this technique has been extended to colloidal systems[4–8] to produce colloidal crystals. This technique is recognized for its high reproducibility and robustness with colloids. To understand the spin-coating of colloids and to extend its commercial applicability, it is necessary to characterize the flow and fluid properties[3,9] as well as the fundamental interactions between the particles and the fluid. The interactions between the colloidal particles have been studied extensively;[10,11] however, the spinning duration is as short as a fraction of a second, and the dynamics lies in fast regimes. Some reports[9,12–14] provide insights into the spin-coating systems that combine the flow and the properties of fluid. Recently, a report on external electric fields while spin-coating a colloid[15] has shown that hydrodynamic flows are affected *via* dielectrophoretic confinement of the suspension that yields colloidal crystals in a predefined direction. In the same period, another report[16] showed the possibility of applying a magnetic field while a superparamagnetic colloid is spin-coated.

Hydrodynamical systems in rotation with magnetic fields are under study in broader areas. For example, this kind of systems may be used as models for astrophysical objects in different stages of their existence. Another relevant issue which is under consideration by the scientific community is thin film preparation using external magnetic fields. However, on the one hand there is no complete agreement about the role played by the solvent of an evaporating suspension during the spin coating. Meyerhofer[2] took the effect of evaporation of the solvent into account for the first time. Several models have been developed that focus on how the rate of evaporation depends on the angular speed ω. This dependency is related to the predominant mechanisms in evaporation, namely the removal of solvent vapor from the 'air' boundary layer, the diffusion of the liquid solvent to the surface of the colloid, *etc.* On the other hand, neither the effect of an applied magnetic field on volatile suspensions of superparamagnetic colloids nor their interplay with fast rotation of the substrate is known. Our results could be applied to other magnetorheological fluids, characteristics of which can be found in a recent review.[17]

In this article, we show that it is possible to compare the thickness of the dried deposits of spin coated colloids under very different conditions. In this first result we do not apply any magnetic field. Other results involve a superparamagnetic colloid with and without applied magnetic field. The model that we develop allows us to obtain the relative variation of the viscosity of the colloid. In the following, we first provide some information regarding the experiments, and then we will present the model. Finally, we report the experimental results and discuss them.

2 Experimental set-up

The experiments were performed in a customized commercial spin-coater at rotation rates from 2000 to 7000 rpm. Magnetic fields ranging from 0 to 0.066 T were applied using a pair of Helmholtz coils which are placed in such a way that the

Dept. of Physics and Appl. Math., University of Navarra, Pamplona, Spain. E-mail: wens@unav.es

† Electronic supplementary information (ESI) available: Characterization of superparamagnetic particles and film thickness profiles. See DOI: 10.1039/c2sm27682h

‡ Present address: Sri Ramakrishna Engineering College, Vattamalaipalayam, NGGO Colony Post, Coimbatore-641 022, India.

substrate spins in the region of uniform axial magnetic field. A sketch of the experimental setup is shown in Fig. 1C and photographs of the spin-coater with Helmholtz coils are shown in Fig. 1A and B. Applied magnetic fields are varied by adjusting the current in these coils with an external power supply.

Glass substrates of size $38 \times 25 \times 1$ mm^3 are used for all experiments. They are cleaned with acetone in an ultrasonic bath for fifteen minutes followed by a soft basic piranha etch which consists of ultra-pure water/ammonia/hydrogen peroxide at the ratio of 5 : 3 : 1 at 67 °C for forty minutes. The substrates are rinsed with ultra-pure water after each cleaning/etch stage. The cleaned substrates are then dried by nitrogen gas blow. Freshly cleaned substrates are used for each experiment.

The particles are superparamagnetic (see ESI†) and consist of silica coated magnetite of diameter 1.51 ± 0.05 μm (density = 1.6–1.8 g cm^{-3}). They are obtained from microParticles GmbH, Germany. The particles are weighed and homogeneously suspended in ultra-pure water to obtain a concentration of 1.44% (v/v). The suspension has an estimated viscosity 3.6% higher than that of ultra-pure water. Experiments which concern this suspension are referred as SiO_2-MAG. The suspension is ultrasonicated for fifteen minutes before commencing experiments. The spin-coater is operated at a required rotation rate ω and the magnetic field H is applied. Then, 120 μl of suspension is pipetted onto the spinning substrate. Once the spun suspension is dried, the field is turned off. Micrographs are taken on the substrates at 2 mm intervals from the center of spinning. After checking that under the same conditions (ω, H) all the deposits are similar, we analyzed one micrograph for each set (ω, H, r), where r is the distance to the center of spinning. Typical micrographs, from experiments performed without magnetic field (Fig. 2A) and with magnetic field (Fig. 2B) are shown. The images are analyzed through home-made routines in Octave. As all the deposits from this experiment are submonolayers we characterize the amount of deposit by the area occupied by clusters of superparamagnetic particles relative to the total area of the region. This value is measured for each micrograph and it is called "occupation factor" or surface coverage ε^2. For comparison, representative micrographs with and without applied field are shown in Fig. 3. Although the elongated clusters clearly appear when a magnetic field is applied, in previous similar experiments it has been proved that they are not oriented.[16]

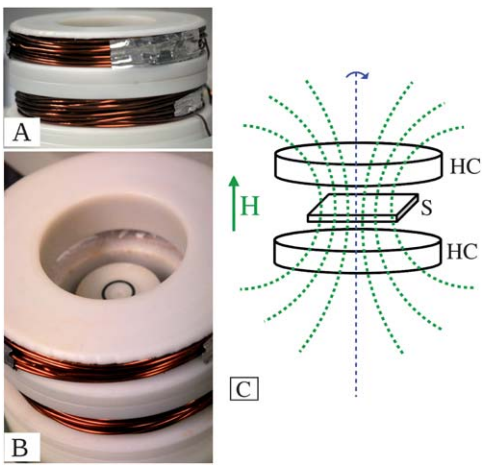

Fig. 1 (A and B) Photographs of experimental components: (A) a pair of Helmholtz coil and (B) the same mounted on a spin-coater. (C) Sketch of the experimental setup and the magnetic field lines (HC: Helmholtz coil; S: substrate). The substrate spins in the region of uniform magnetic field.

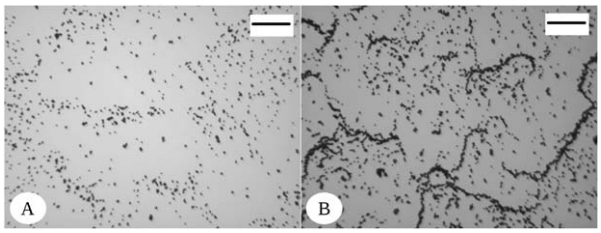

Fig. 2 Micrographs of spin-coated substrate at 8 mm from the center of spinning. Scale bars are 50 μm. (A) $H = 0$ and (B) $H = 0.066$ T. Spinning rate is 5000 rpm. When the magnetic field is applied, the superparamagnetic particles accumulate together to form elongated clusters.

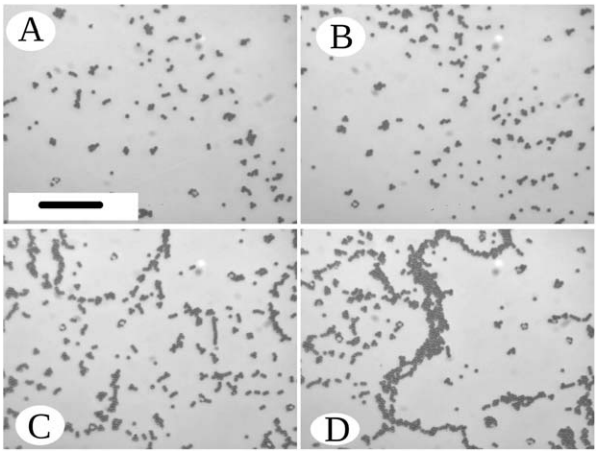

Fig. 3 Higher resolution micrographs of the spin-coated substrate. The spinning rate is 5000 rpm and the scale bar is 25 μm. (A and B) $H = 0$ and (C and D) $H = 0.066$ T.

To check the validity of the model (see below) we consider a reference experiment, whose results were reported by Giuliani *et al.*[18] They used plain silica particles with a diameter of 458 nm suspended in Methyl Ethyl Ketone (MEK). The concentration was 20% (v/v). They spin-coated the non-magnetic colloid without magnetic field at various spinning rates. Results concerning this experiments are referred as SiO_2-NM.

3 Model

3.1 Previous results

In 1958, Emslie *et al.*[1] reported a model of spin-coating without evaporation. That model accounts for (a) the viscous forces caused by the fluid properties and (b) the centrifugal forces of spinning. When a polymer solution is spun, it leaves a thin layer indicating that the solvent has evaporated. To account for evaporation, Meyerhofer[2] included a correction based on the

assumption that the spin-coating process consists of two different stages: (a) a flow dominated phase followed by (b) an evaporation dominated phase. There are reports[19,20] that further characterize the fluid flow of non-Newtonian liquids. Later on, Cregan and O'Brien[21] considered that the solvent evaporation is simultaneous with the flow dominated phase because the solvent starts to evaporate once the suspension is pipetted on to the spinning substrate. Although the Cregan model is more sophisticated, it assumes a constant evaporation rate E. That is, E is not considered to depend on the rotation rate ω. In other models,[2,9] it is assumed that $E \propto \omega^{\frac{1}{2}}$ or $E \propto \omega$.

In the Cregan model, the deposited layer thickness ($h_\infty^{(s)}$), where the s superscript indicates 'solute' and '∞' means at long times, *i.e.* when the colloid is dried on the substrate, is given by:

$$h_\infty^{(s)} = \frac{h_0^{(s)}}{h_0^{(l)}}\left(\frac{E}{\alpha}\right)^{\frac{1}{3}}, \tag{1}$$

where $h_0^{(s)}$ and $h_0^{(l)}$ are the initial solute and the solvent thickness, respectively. The measurable quantity is the initial film thickness $h_0^{(s)} + h_0^{(l)}$. Also, in eqn (1), $\alpha = \frac{2\omega^2}{3\nu}$ where ω is the spinning rate and ν is the kinematic viscosity of solvent. E, as mentioned above, corresponds to the evaporation rate of the solvent.

It is assumed that the initial suspension is homogeneous. Then, the thicknesses can be converted into volumes and hence $\frac{h_0^{(s)}}{h_0^{(l)}} = \frac{C}{1-C}$, where C is the initial concentration in v/v. Eqn (1) thus becomes:

$$h_\infty^{(s)} = \frac{C}{1-C}\left(\frac{3}{2}\nu E\right)^{\frac{1}{3}}\omega^{-\frac{2}{3}} = A\omega^{-\beta}, \tag{2}$$

where A is a constant over the experiment and $\beta = \frac{2}{3}$.

3.2 Spin-coating of a colloid

We assume that the solvent is volatile enough, such that the characteristic time in which appears an appreciable gradient of concentration due to the centrifugal force is smaller than the experiment duration. Consequently, the suspension volume elements move as a whole and the discrete nature of the deposited colloidal particles can be taken into account by the use of a compact equivalent height (CEH). The CEH is defined as the thickness of a homogeneous layer whose volume is the same as the particles deposited (Fig. 4).

Under this assumption we may use a continuum valid model just by substituting the thickness of the deposited homogeneous layer with the CEH. So, from now on, we are going to use $h_\infty^{(s)}$ as the valid notation in colloidal spin-coating. Of course, the thickness could be dependent on the distance to the center of rotation r (non-planarization).[18] Thus, the definition has to be properly extended to a local one. Nevertheless, in this section we are going to consider a constant thickness.

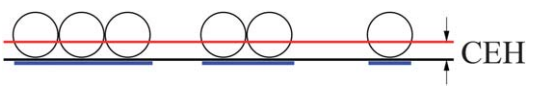

Fig. 4 Sketch for the meaning of the compact equivalent height (CEH) of a deposit.

In the case of submonolayers formed by 2-D hexagonal structured clusters, which is a good approximation for non-chained clusters,

$$h_\infty^{(s)} = \frac{2\pi}{3\sqrt{3}}R\varepsilon^2, \tag{3}$$

where R is the radius of the colloidal particles. The coefficient of ε^2 comes from geometric considerations.

In the case of multilayers, the CEH is proportional to the number of layers n, as each layer accounts for the number of particles per unit area. The coefficient of n is also of geometric nature and depends on the microscopic structure and orientation. It is assumed that the most common structures in spin coating of colloids correspond to the most close packed ones (fcc and hcp).[5–8] For the case of fcc_{100} it can be straightforwardly proven that $h_\infty^{(s)} = \frac{2\pi}{6}Rn = \frac{\pi}{3\sqrt{2}}h^* + (1-\sqrt{2})\frac{2\pi}{6}R$. For the case of hcp, $h_\infty^{(s)} = \frac{2\pi}{3\sqrt{3}}Rn = \frac{\pi}{3\sqrt{2}}h^* + \left(1-\sqrt{\frac{3}{2}}\right)\frac{2\pi R}{3\sqrt{3}}$. In both cases h^* is the dimensional thickness of the deposit.

For a large number of layers ($n \gg 1$), in general $h_\infty^{(s)} \approx \mathrm{APF} \times h^*$, where APF is the atomic packing factor for the structure. In the case of fcc and hcp:

$$h_\infty^{(s)} \approx \frac{\pi}{3\sqrt{2}}h^*. \tag{4}$$

3.3 Scaling of thicknesses of colloidal deposits under different conditions

To compare two experiments that follow the same continuum model, but performed under different conditions, it is possible to compute the ratio between both CEH. In the most complex case of one being a multilayer-reference and the other being a monolayer:

$$\frac{h_\infty^{(s,ref)}}{h_\infty^{(s)}} = \frac{1}{2}\sqrt{\frac{3}{2}}\,\frac{h_{ref}^*}{R\varepsilon^2}, \tag{5}$$

where R is the radius of the particles of the submonolayer. Here, the left hand side of the equation can be substituted by the considered model. If we want to compare an experiment which gives a submonolayer to the height of a reference experiment h_{ref}^* in a graph, we should plot also the scaled height for the submonolayer h_{scaled}:

$$h_{scaled} = 2\sqrt{\frac{2}{3}}R\varepsilon^2\frac{h_\infty^{(s,ref)}}{h_\infty^{(s)}}, \tag{6}$$

which in the case of the Cregan model becomes:

$$h_{scaled} = 2\sqrt{\frac{2}{3}}R\varepsilon^2\frac{A_{ref}}{A}. \tag{7}$$

3.4 Magnetorheology

In this subsection, we generalize eqn (2) by including an evaporation rate that may depend on ω, but not on the magnetic field.

Now we compare two experiments performed under the same conditions except for the applied magnetic field, which both lead to submonolayers. We compare them, as before, by computing the ratio of the corresponding CEH. In the case of one without magnetic field and the other with applied magnetic field:

$$\frac{h_{\infty}^{(s)}(H,\omega)}{h_{\infty}^{(s)}(H=0,\omega)} = \frac{\varepsilon^2(H,\omega)}{\varepsilon^2(H=0,\omega)}. \quad (8)$$

If we substitute the left hand side of eqn (8) by the corresponding generalized Cregan equation, the only parameter which remains dependent on the field is the kinematic viscosity ν. This leads to:

$$\frac{\nu(H,\omega)}{\nu(H=0,\omega)} = \left[\frac{\varepsilon^2(H,\omega)}{\varepsilon^2(H=0,\omega)}\right]^3 \quad (9)$$

4 Results and discussion

4.1 Occupation factor and non-planarization

From the spin-coated substrates, micrographs are taken at 2 mm increasing intervals from the center of spinning (r). Representative micrographs are shown in Fig. 2. The micrographs are thresholded, segmented and then analyzed through homemade routines in Octave. For each micrograph we calculate the occupation factor ε^2. Plots of the occupation factor at a spinning rate of 5000 rpm for different magnetic field strengths are shown in Fig. 5. In general, it depends on r as the volatile colloidal suspensions do not planarize.[18] Nevertheless, as the rotation rate increases, the non-planarization becomes less evident. For a given spinning rate, mean occupation factors are calculated for the different applied magnetic fields and they are used for further analysis.

4.2 Film thickness and comparisons with models

Without applied magnetic field. As has been already mentioned, we compare our results to the reference experiment (SiO_2-NM) reported by Giuliani *et al.*[18] In order to overcome the non-planarization, we use a spatial average of the final deposit thickness, which was measured utilizing Atomic Force Microscopy (Fig. 4a of the reference experiment letter[18]). This thickness (h^{*}_{ref}) corresponds to a multilayer because the suspension is concentrated enough, and it is plotted as a function of ω, represented by circles in Fig. 6. Using eqn (7), the scaled thickness for the deposits of SiO_2-MAG experiments is calculated and plotted, with squares, in Fig. 6. The deposits of SiO_2-MAG correspond to submonolayers because the suspension is dilute enough. Standard deviation in each value characterizes the non-planarization phenomenon. In the ESI,† results corresponding to other conditions are compared to SiO_2-NM and SiO_2-MAG and show good agreement.

Although particles and solvents have very different characteristics (as detailed the experimental set-up section), data from both experiments collapse onto a single curve. The common curve represents a decreasing tendency for deposit thickness as the spinning rate is increased. The deviation from the common curve at high angular speeds (7000 rpm) may come from the fact that, as the solvent for the SiO_2-MAG (water) is more viscous and less volatile, there is shear thickening behavior with respect to the SiO_2-NM case (suspension in MEK).

We compare the correlated experimental data with appropriate models.[2,9,21] Our experimental data are in good agreement with all these models within the experimental error, see squares and big circles in Fig. 7. As said above, irrespective of the nature and the kind of suspension, the final deposit thickness depends on the spinning rate ω. Power-law fit to the non-magnetic SiO_2-NM reference experiment shows a strong dependency on the spinning rate, $\omega^{-\frac{3}{4}}$ (Fig. 7 – solid line). The exponent value is

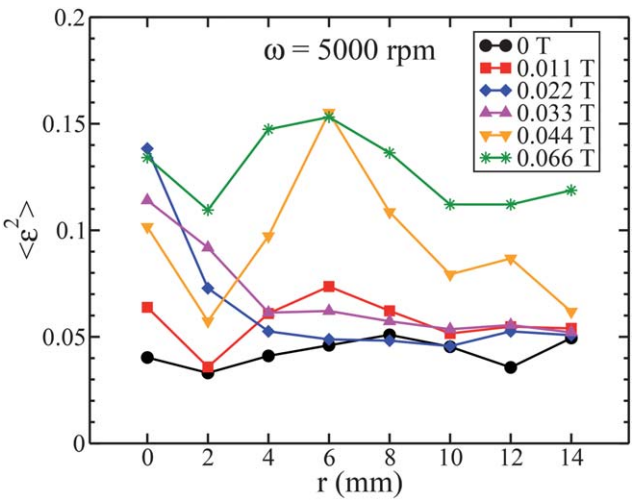

Fig. 5 Occupation factor as a function of increasing radial distance from the center of spinning. Spinning rate is 5000 rpm. The estimated error for these data is of the order of 0.02.

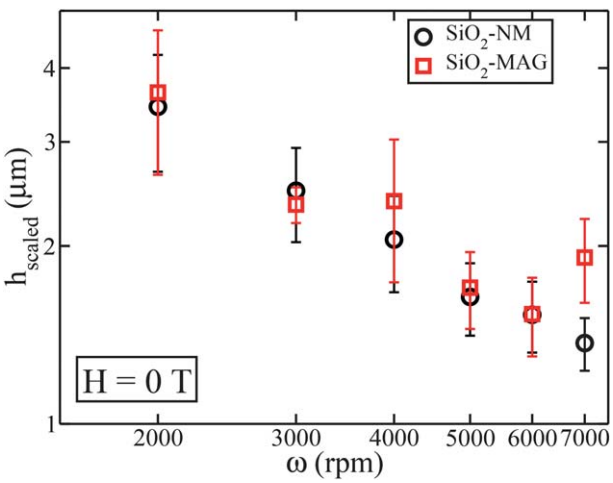

Fig. 6 Comparison of the film thickness profile for different colloids without applied magnetic field. Squares: SiO_2-MAG; circles: SiO_2-NM. For the latter case, the information is extracted from Fig. 4a of the reported[18] reference experiment by doing a spatial average. Data from both experiments seem to collapse onto a single curve.

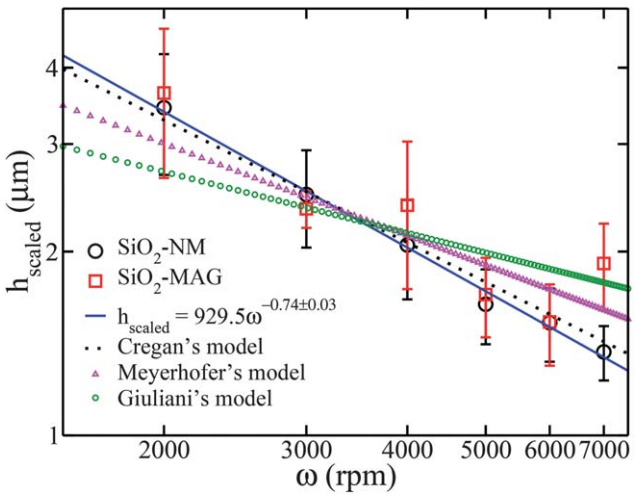

Fig. 7 Comparison of the film thickness profiles for different suspensions with models. Squares: SiO_2-MAG; big circles: SiO_2-NM. For the big circles, the information is extracted from Fig. 4a of the reported[18] reference experiment by doing a spatial average. The data from both experiments collapse onto a single curve. The solid line is the best power-law fit to the SiO_2-NM reference experiment. The data from experiments are compared with the relevant models.[2,9,21] The dotted line corresponds to the model proposed by Cregan and O'Brien.[21] Triangles represent the model from Meyerhofer[2] and the small circles are obtained using the model reported in ref. 9.

close to the reported one $\left(-\frac{2}{3}\right)$, in the model proposed by Cregan and O'Brien.[21] Nevertheless, the other considered models could also be valid.

With applied magnetic field. On applying a magnetic field while spin-coating, the scaled thickness for the deposits of SiO_2-MAG experiments decreases as the spinning rate is increased. In Fig. 8, for clarity, one case corresponding to the field condition is plotted using diamonds. In this situation too the decreasing tendency of the scaled thickness depends on the spinning rate; however, the thickness value for a given spinning rate is higher (diamonds in Fig. 8) than the ones obtained without magnetic field (squares in Fig. 8). This indicates an increase in mean occupation factor when a field is applied. The magnetic dipole interactions of the superparamagnetic particles increase the effective viscosity of the suspension,[16] which in turn increases the mean occupation factor. The even increase of the mean occupation factor at low fields indicates that the main effect of the magnetic field is to increase the effective viscosity of the superparamagnetic colloid.

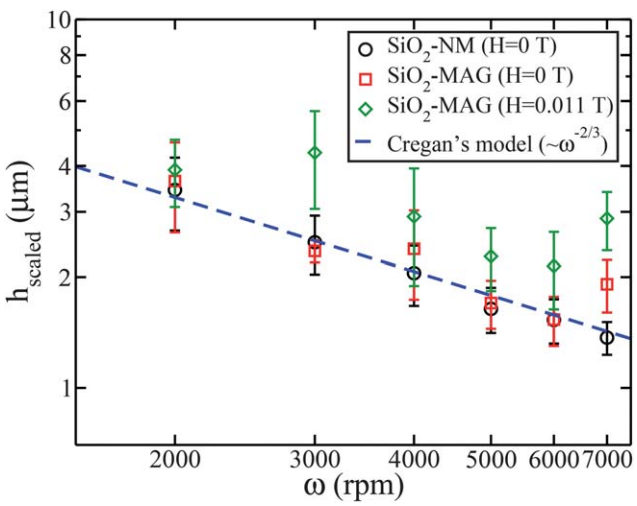

Fig. 8 Comparison of the film thickness profiles for different colloids without and with applied magnetic field. Squares: SiO_2-MAG, $H = 0$ T; diamonds: SiO_2-MAG, $H = 0.011$ T; circles: SiO_2-NM. For circles, the information is extracted from Fig. 4a of the reported[18] reference experiment by doing a spatial average. Dashed line is a comparison to Cregan model.

4.3 Magnetorheology

Using eqn (9), the relative change in viscosity due to the applied field can be calculated. This equation is independent of the model which assumes the compact equivalent height. As stated above, we generalize the equation reported by Cregan and O'Brien[21] so that the evaporation of solvent may depend on the spinning rate. Information regarding the occupation factor can be obtained directly from the SiO_2-MAG experiments (with and without magnetic fields, respectively). We plot the mean and standard deviation for relative change in viscosity for all ω as shown in Fig. 9. The standard deviation in the form of error bar appears due to the varying spinning rate and each value emphasizes the critical role played by ω. Nonetheless, one can relate a larger standard deviation to a more relevant non-Newtonian character[5,22,23] as the applied fields are increased. The mean relative viscosity is larger with the field. This is through the magnetic dipole interactions between the superparamagnetic particles.[16] At high magnetic fields, more particles accumulate in elongated clusters. Morphological transition from sparse (without magnetic field) to sub-monolayer deposits (with magnetic field) of superparamagnetic particles can be seen in Fig. 2 and 3. Under similar experimental conditions, we did not observe any preferred direction for these clusters[16] and orienting them in a desired direction is challenging.

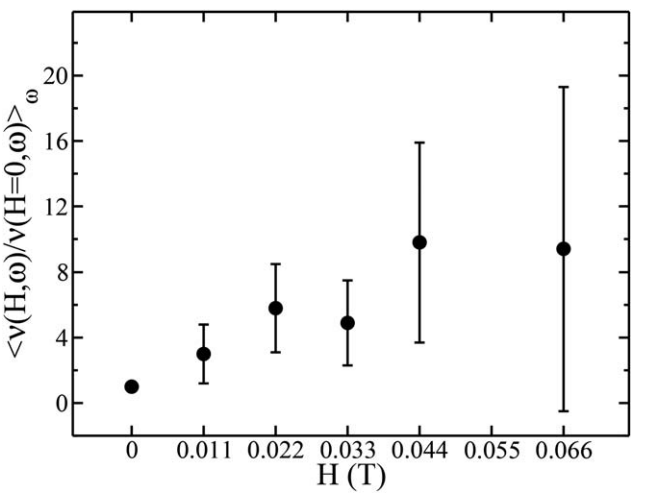

Fig. 9 Relative change in the viscosity for all spinning rates, in the form of mean value and standard deviation, as a function of the applied magnetic fields.

5 Conclusions

In the absence of a magnetic field we prove that it is possible to compare results from experiments under very different conditions under a common frame; at least for the thicknesses of the colloidal deposits. We were able to introduce a Compact Equivalent Height that allows us to extrapolate results from classical spin-coating to colloidal spin-coating.

We observe that the main effect of the magnetic field on a suspension made of superparamagnetic particles and volatile solvents is the formation of clusters of irregular shapes and of chain-like shapes. The latter are advected by the strong flows of the spin-coating process, which randomize the cluster orientations. Consequently, we can only observe a change of the rheological properties of the system.

Our experiments could provide indications on the structure formation mechanisms while using the spin-coating method with colloids. To understand these mechanisms, the phenomena occurring at concentrations corresponding to the transition from submonolayers to multilayers should be studied; this work is in progress.

We also were able to measure the relative viscosity when a magnetic field is applied, and the overall change in the non-Newtonian character of the suspension. This technique could be applied to other magnetorheological fluids, where we may recover already known behaviors.[24] As the future of magnetorheological fluids is very promising,[17] to support the broad application of this method independent measurement of the field-dependent viscosity under shear stresses could be initiated. Established methods such as rheological microscopes[25–27] can be employed but the presence of external magnetic fields during the measurement is challenging.

Acknowledgements

We thank A. Irigoyen Barrio for his help in preparing the colloidal suspension. We acknowledge C. Gómez-Polo for her generous loan of SQUID and fruitful discussions, and J.M. Pastor and M.A. Miranda for the magnetic characterization of the superparamagnetic colloidal particles. We thank Claire F. Woodworth for her help in correcting grammar mistakes while preparing the manuscript. This work is partly supported by the Spanish Government Contract no. FIS2011-24642. M. P. acknowledges the financial support from the "Asociación de Amigos de la Universidad de Navarra" and the Management, Sri Ramakrishna Engineering College, Coimbatore, India.

References

1 A. G. Emslie, F. T. Bonner and L. G. Peck, *J. Appl. Phys.*, 1958, **29**, 858–862.
2 D. Meyerhofer, *J. Appl. Phys.*, 1978, **49**, 3993–3997.
3 D. Birnie III and M. Manley, *Phys. Fluids*, 1997, **9**, 870–875.
4 P. Jiang and M. McFarland, *J. Am. Chem. Soc.*, 2004, **126**, 13778–13786.
5 L. Shereda, R. Larson and M. Solomon, *Phys. Rev. Lett.*, 2008, **101**, 16–19.
6 C. Arcos, K. Kumar, W. González-Viñas, R. Sirera, K. M. Poduska and A. Yethiraj, *Phys. Rev. E: Stat., Nonlinear, Soft Matter Phys.*, 2008, **77**, 050402(R).
7 A. Mihi, M. Ocaña and H. Míguez, *Adv. Mater.*, 2006, **18**, 2244–2249.
8 M. Pichumani, P. Bagheri, K. M. Poduska, W. González-Viñas and A. Yethiraj, *Soft Matter*, 2013, DOI: 10.1039/c3sm27455a.
9 M. Giuliani, Ph.D. thesis, University of Navarra, 2010.
10 A. Yethiraj and A. van Blaaderen, *Nature*, 2003, **421**, 513–517.
11 A. Yethiraj, *Soft Matter*, 2007, **3**, 1099–1115.
12 D. E. Bornside, C. W. Macosko and L. E. Scriven, *J. Appl. Phys.*, 1989, **66**, 5185–5193.
13 B. G. Higgins, *Phys. Fluids*, 1986, **29**, 3522.
14 T. J. Rehg and B. G. Higgins, *AIChE J.*, 1992, **38**, 489.
15 A. P. Bartlett, M. Pichumani, M. Giuliani, W. González-Viñas and A. Yethiraj, *Langmuir*, 2012, **28**, 3067.
16 M. Pichumani and W. González-Viñas, *Magnetohydrodynamics*, 2011, **47**, 191.
17 B. J. Park, F. F. Fang and H. J. Choi, *Soft Matter*, 2010, **6**, 5246–5253.
18 M. Giuliani, W. González-Viñas, K. M. Poduska and A. Yethiraj, *J. Phys. Chem. Lett.*, 2010, **1**, 1481–1486.
19 A. Acrivos, M. J. Shah and E. E. Petersen, *J. Appl. Phys.*, 1960, **31**, 963.
20 S. A. Jenekhe and S. B. Schuldt, *Ind. Eng. Chem. Fundam.*, 1984, **23**, 432.
21 V. Cregan and S. O'Brien, *J. Colloid Interface Sci.*, 2007, **314**, 324.
22 N. J. Wagner and J. F. Brady, *Phys. Today*, 2009, **62**, 27.
23 X. Cheng, J. H. McCoy, J. N. Israelachvili and I. Cohen, *Science*, 2011, **333**, 1276.
24 F. F. Fang, H. J. Choi and M. S. Jhon, *Colloids Surf., A*, 2009, **351**, 46–51.
25 D. T. Chen, E. R. Weeks, J. C. Crocker, M. F. Islam, R. Verma, J. Gruber, A. J. Levine, T. C. Lubensky and A. G. Yodh, *Phys. Rev. Lett.*, 2003, **90**, 108301.
26 D. T. Chen, Q. Wen, P. A. Janmey, J. C. Crocker and A. G. Yodh, *Annu. Rev. Condens. Matter Phys.*, 2010, **1**, 301.
27 K. N. Nordstrom, E. Verneuil, P. E. Arratia, A. Basu, Z. Zhang, A. G. Yodh, J. P. Gollub and D. J. Durian, *Phys. Rev. Lett.*, 2010, **105**, 175701.